ASTROBIOLOGY
Volume 20, Number 8, 2020

DOI: 10.1089/ast.2020.2228

Estimated Minimum Life Span of the Jezero Fluvial Delta (Mars)

Francesco Salese,[1,2] Maarten G. Kleinhans,[1] Nicolas Mangold,[3] Veronique Ansan,[3] William McMahon,[1] Tjalling de Haas,[1] and Gilles Dromart[4]

Abstract

The paleo-lake floor at the edge of the Jezero delta has been selected as the NASA 2020 rover landing site. In this article, we demonstrate the sequences of lake filling and delta formation and constrain the minimum life span of the Jezero paleo-lake from sedimentological and hydrological analyses. Two main phases of delta evolution can be recognized by utilizing imagery provided by the High Resolution Imaging Science Experiment (NASA Mars Reconnaissance Orbiter) and High Resolution Stereo Camera (ESA Mars Express): (1) basin infilling before the breaching of the Jezero rim and (2) the delta formation itself. Our results suggest that delta formation occurred over a minimum period of 90–550 years of hydrological activity. Breaching of the Jezero rim occurred in at least three distinct episodes, which spanned a far longer time-period than overall delta formation. This evolutionary history implies that the Jezero-lake floor would have been a haven for fine-grained sediment accumulation and hosted an active environment of significant astrobiological importance. Key Words: Jezero fan-delta—Lake—Mars—Landing site—Fluvial activity—Neretva Vallis. Astrobiology 20, 977–993.

1. Introduction

Remnants of ancient deltas provide a critical record of ancient surface flow on Mars. Interpretations of these sedimentary archives are of fundamental importance for quantifying the hydrological history of the planet (Salese *et al*., 2020). A range of delta types have so far been recognized (Di Achille and Hynek, 2010; Hauber *et al*., 2013; Salese *et al*., 2019), including simple stepped deltas (Irwin III *et al*., 2005; Di Achille *et al*., 2006; Weitz *et al*., 2006; Kraal *et al*., 2008; Hauber *et al*., 2013; Salese *et al*., 2019), complex and lobate deltas (Pondrelli *et al*., 2008; Mangold *et al*., 2012; Hauber *et al*., 2013; Salese *et al*., 2016), and Gilbert-type deltas (Ori *et al*., 2000; Di Achille *et al*., 2007; Hauber *et al*., 2013; Salese *et al*., 2019). Whereas stepped deltas are readily explained by a single outflow event (Kraal *et al*., 2008; de Villiers *et al*., 2013), many studied systems are far more complex because they have much greater catchment areas and often relate to breached craters. The Jezero crater delta, along with Moa Valles-Liberta (Salese *et al*., 2016), Eberswalde crater (Malin and Edgett, 2001; Pondrelli *et al*., 2008; Mangold *et al*., 2012), and Sabrina and Hypanis (Adler *et al*., 2018), is among the few martian deltas with evident stratigraphy, avulsing channels, and multilobate depositional patterns. Previous studies have yielded conflicting estimates of the timescale of evolution within the Jezero delta, with the total duration of hydrological activity ranging from mere decades to upward of millions of years (Fassett and Head, 2005; Ehlmann *et al*., 2008; Schon *et al*., 2012; Goudge *et al*., 2015). Notably, it remains unclear whether delta formation occurred during extended epochs of clement climatic conditions (*i.e.*, favorable for life) or during punctuated intervals of allogenically forced sedimentary events (*e.g.*, regional impacts, volcanism, or tectonics) (Brakenridge *et al*., 1985; Hauber *et al*., 2013; Halevy and Head, 2014). This latter hypothesis would imply that lake conditions may have been similar to those of the present day and thus were likely prohibitive for life.

The aims of this article are (a) to re-examine the delta-forming discharge from the Neretva Vallis; (b) to consider the active lake's water supply and loss mechanics; and (c) to determine the geologic timescale of delta formation.

Utilizing high-resolution digital elevation models (DEMs), we estimated the systems' hydrological potential and propose different scenarios of evolution with varied key sediment transport parameters (*e.g.*, grain size). Sediment transport predictions are intricately linked to estimates of grain size, channel depth, and gradients, such that minor

[1]Faculty of Geosciences, Utrecht University, Utrecht, The Netherlands.
[2]International Research School of Planetary Sciences, Università Gabriele D'Annunzio, Pescara, Italy.
[3]Laboratoire de Planétologie et de Géodynamique de Nantes, UMR6112, CNRS/Nantes University, Nantes, France.
[4]University of Lyon, ENSL, University of Lyon 1, CNRS, LGL-TPE, Lyon, France.

differences in input conditions may result in sediment budget outputs orders of magnitude apart (perhaps explaining the contradictory estimates of Jezero crater evolution predicted by previous researchers (Fassett and Head, 2005; Ehlmann *et al*., 2008; Schon *et al*., 2012; Goudge *et al*., 2015) (Fig. 1). Despite imbedded (and unavoidable) uncertainties, physics-based predictors (used in this work, rather than empirically based estimates) provide the most robust flow and transport rates available. Empirically derived hydrological estimates that assume fixed sediment concentrations (Moore *et al*., 2003; Irwin *et al*., 2004, 2015; Mangold *et al*., 2012) may yield incorrect estimates of system duration due to the following: (1) considering the power law-dependence of sediment flux on flow shear stress, a simplistic assumption can be wrong by several orders of magnitude, while physics-based methods are always within two orders of magnitude even with a large uncertainty of original grain size. (2) Sediment concentration values applied by previous authors are relatively high and imply unrealistic hyperconcentrated flows (considering the low-gradient slopes and probable hinterland conditions). Morphometry, valley topography, and discharge rates of channels and their stratigraphic relationships with lithological units of origins other than the fluvial and lacustrine are investigated in a companion article (Mangold *et al.*, 2020).

1.1. Jezero crater context

Jezero is a 50-km-diameter crater with a volume of 463 km^3. It is a shallow impact basin with a major channel system cutting its western rim. The crater contains a large irregular fan deposit with a minor channel entering from the north (Fassett and Head, 2005) (Fig. 2a). We model the contribution to the crater infilling and delta formation of the western main valley, and we analyze the breach evolution at the eastern side of the crater. The northern valley does not contain evidence of fan deposition and is overall poorly developed. The crater is breached on the eastern side where there is a connected erosive channel network (Fig. 1). The maximum elevation inside the crater basin, which water may have reached, is −2243 m (Fig. 2: Profile R–S). Both the elevation of the delta front and the bottom of the breach are −2410 m (Fig. 2: Profiles O–Q and R–S). All parameters (delta surface, volume gradient, eroded sediment valley volume, crater rim diameter, observed depth below rim peak, volume of the breach) were accurately delineated through our DEMs (see Section 2). The observed depth below the rim peak in this case matches with highest breaching point at −2243 m below the Mars datum. Nevertheless, particular deltaic subenvironments (*e.g.*, offshore delta toe-sets) have been eroded, with this missing geomorphic evidence potentially leading to underestimates of the total active duration for the Jezero system.

2. Methods

2.1. General approach

We use established hydrological and sediment transport predictors that are well tested for terrestrial conditions and corrected for martian gravity (Kleinhans, 2005). The principle of these formative timescales is that flows require a certain minimum duration to work (*i.e.*, remove, transport, or deposit a known sediment volume) and must involve a certain volume of water that is sometimes constrained in nonoverflowing lakes (Kleinhans, 2005; Roda *et al*., 2014). While flow and sediment transport predictors undoubtedly simplify reality, the timescales of morphology development are rather well constrained by this methodology. We use these predictors to estimate the duration of the Jezero fluvial system, and we further test it on well-constrained terrestrial (Holocene) cases, including the Wax Lake Delta (WLD) and Lake Constance, to corroborate general validity [previously assessed by Duller *et al*. (2015)]. To obtain a range of possible predictions, we simulated a number of conditions for the most uncertain and sensitive variables (*i.e.*, grain size and channel dimensions). Channel width and slope can be derived from visible images and DEMs both for terrestrial (WLD and Lake Constance) and martian (Jezero delta) examples. Channel depth can be directly measured on Earth and estimated on Mars by using DEMs (with indications for original water depth ranging between preserved terrace height and bank-full flow conditions). Flow velocity was estimated by using a friction law and a measured depth from altimetry data. Channel width, depth, and slope were carefully measured by using High Resolution Imaging Science Experiment (HiRISE) DEMs for the Jezero delta [in addition to the Jezero breach because over- or underestimating depth not only affects derived discharge but also indirectly the velocity; through the roughness equation, see Kleinhans (2005)]. Sediment flux is calculated by using two methods: one that assumes a bed load-dominated transport (with mostly rolling and saltating particles and limited energy) and another that assumes a suspended load-dominated event (noncohesive granular material). The sediment mobility, which depends on flow and sediment properties, is used to determine which of the two transport modes is most valid. In such a system, suspended/bed load transport ratio is far larger than one, so classic suspension-dominated sediment transport capacity predictors are used that are corrected for martian conditions (Kleinhans, 2005). Models are based on steady and uniform flows equal to the water surface slope and channel bed surface slope.

In this article, we assume, based on morphological evidence (terraces), a constant (5 m deep) bank-full discharge. While it is likely that some form of hydrograph is more representative of original flow conditions, the combination of the magnitude/frequency relation of flow and the nonlinearity of sediment transport renders the average sediment transport rate closer to the bank-full discharge than high-peak variance. This is due to the fact that the most extreme discharges (while transporting disproportionally more sediment) are quite rare, while the lowest discharges (while perhaps much more common than the bank-full condition) induce little sediment transport. These assumptions are in agreement with observations that the resulting channel dimensions scale well to bank-full discharge as a measure for the channel forming discharge of fluvial channels (Leopold *et al.*, 1964).

We assume transport of one sediment size, whereas in reality there would have been a mixture. In particular, the Jezero delta is likely composed of a range of grain sizes, as suggested by the interior of the delta, which shows variations between the supposed point bar, likely sand facies and

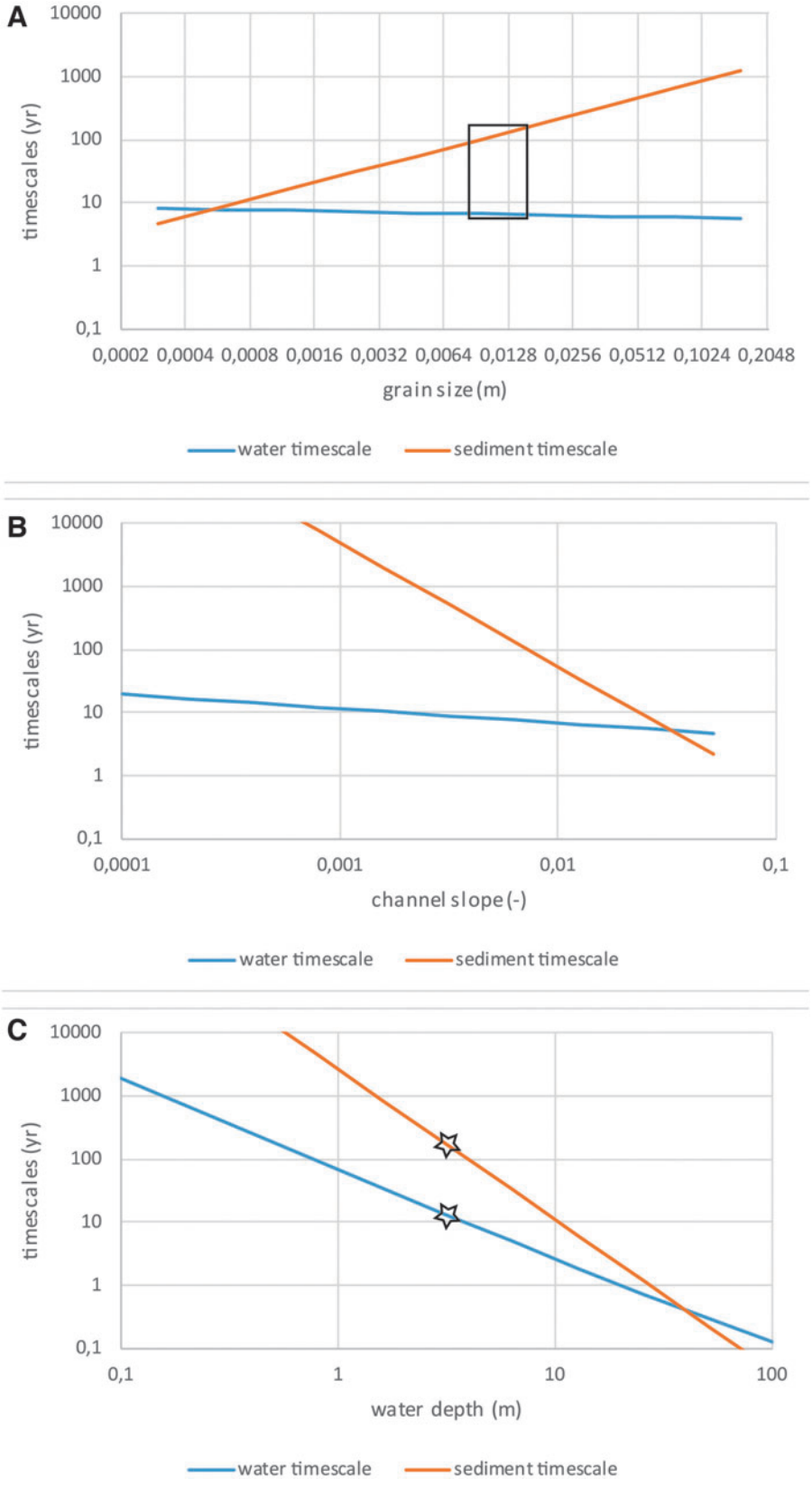

FIG. 1. Main parameters (grain size, channel slope, channel depth) used in the hydrological modeling that strongly affect the transport predictors. **(A)** Grain size versus timescale. Based on different grain sizes, the blue line indicates the amount of time needed to fill the basin, whereas the orange line displays the timing to form the delta. The black box indicates the grain size range that we considered to estimate the Jezero timing (see main text). **(B)** Channel slope versus timescale. The slope is a crucial parameter for estimating delta timescale, as is evident from this plot. Reducing the slope by a factor of 10 implies a timescale reduction by a factor of 100. Careful and high-resolution estimates of the channel slope are fundamental to better constrain the timescale of the Jezero paleo fluvio-lacustrine system. **(C)** Channel depth versus timescale. Transport predictors are very sensitive to this parameter, reducing the slope by a factor of 10 implies a timescale reduction by a factor of 100. The black stars indicate the 5 m channel depth that we measured through the HiRISE DEM, which we used for the timing estimate. DEM, digital elevation model; HiRISE, High Resolution Imaging Science Experiment.

the inverted channels above. We modeled scenarios for a range of grain sizes to bracket possible conditions (Table 1). Furthermore, many terrestrial deltas develop floodplains and toe-sets from fine material transported as washload, which is the part of the suspended load that is composed of particle sizes smaller than those found in appreciable quantities in the bed material. It is in near-permanent suspension and, therefore, is transported through the stream without deposition. This washload cannot be determined from the capacity predictors because it is supply-limited from the hinterland rather than capacity-limited by flow. Furthermore, using the water balance we calculate discharge for basin infilling, but we cannot measure the evaporation or pan-evaporation rate due to the lack of paleo-climate parameters on Mars, or the rate of outflow above −2243 m elevation due to the subsequent erosion of the crater rim.

2.2. Data

Data used in this study include all types of visible images acquired for this basin, especially High Resolution Stereo Camera images [HRSC, 12.5 m/pixel, Neukum *et al*. (2004)], Context images [CTX, 6 m/pixel, Malin *et al*. (2007)], and HiRISE images [25 cm/pixel, McEwen *et al*. (2007)]. Mosaics of these data sets have been assembled in a geographic information system (GIS) enabling morphometric measurements. The basin topography has been obtained from CTX and HiRISE DEMs; Neretva Vallis values were estimated throughout HiRISE DEMs (1 m/pixel resolution).

2.3. Case study

We calculated minimum formation times for the Jezero deltas and basin infilling as a function of channel width, depth, and grain size. Formation times were based on predicted water and sediment discharges in comparison with observed lake volume and erosion and deposition volumes. For the Jezero delta in particular (Mars), we used channel depth of 5 m and two different values for channel width: 190 and 50 m. The first value is measured by using the HiRISE DEM, and the second is from the work of Fassett and Head (2005). This second width value is merely applied to demonstrate the sensitivity of the model to width parameter (and in doing so allows application of a more conservative estimate of channel width). The only absolute value of martian grain size was obtained from alluvial fan material inside Gale crater (Williams *et al*., 2013). Evidently inappropriate for application at Jezero, we present in this study a range of different D50 values, from fine sand (0.25 mm) to pebble (20 mm). For the D90 value, we used the relation 5*D50 (Kleinhans *et al*., 2010). Sediment and water discharges were derived from the river morphometric parameters by using Supplementary Data S1 (Kleinhans, 2005) based on the equations listed in the work of Kleinhans (2005). We then discussed and estimated the longevity of deposition as a function of the inlet (Neretva Vallis) and outlet balance, making comparisons with prior works (Fassett and Head, 2005; Ehlmann *et al*., 2008; Schon *et al*., 2012; Goudge *et al*., 2015).

With respect to previous martian analog studies applying the same model (Kleinhans, 2005; Kleinhans *et al*., 2010), our approach is more representative of actual deltaic deposition as we used CTX and HiRISE DEMs to measure width, depth, bed load transport, sediment slope failure of the Neretva Vallis, and terrestrial analogues unaffected by tidal processes. This allows us to use more accurate input parameters than those applied in previous studies (Kleinhans, 2005; Kleinhans *et al*., 2010), particularly for river depth, which is one of the most important parameters that affect the sediment transport process and is difficult to constrain on the basis of erosional channel topography alone (Marra *et al*., 2014). High-resolution topographic data also enable more accurate geological and hydrological analyses, yielding predictions closer to those of typical rivers on Earth.

2.4. Model validation

Model validation was already presented in the work of Kleinhans (2005) for terrestrial and experimental systems, including the Mackenzie and Rhine (NL) (Berendsen and Stouthamer, 2000; Hill *et al*., 2001). The methodology and the equation introduced by Kleinhans (2005) were then implemented by Hoke *et al*. (2011) to assess timescales of formation for seven of the largest ancient martian valley networks. The model was also used on Mars by Mangold *et al*. (2012) and Adeli *et al*. (2016), with an aim of understanding the timescale of evolution of the Eberswalde delta and the fluvial system in Terra Cimmeria, respectively. de Villiers *et al*. (2013) tested the method directly for experimental crater lake deltas and Marra *et al*. (2014) showed it was additionally applicable to erosive experimental systems, and was further supported by a uniquely well-constrained erosional valley case on Mars: the Aram Chaos side valley to Ares Valles (Roda *et al*., 2014). More recently, the abovementioned model used was applied to reconstruct the timescale of formation of the several martian deltas (Kleinhans, 2005; Kleinhans *et al*., 2010) and has already been validated on Earth by Duller *et al*. (2015), who applied it to reconstruct the timescales of the 1918 catastrophically formed fan in southern Iceland (Duller *et al*., 2008, 2014). The real known duration of this event was 6–10 h, and the timescale predicted by their modeling is between 2 and 17 h. Furthermore, to strengthen their test, they modeled several hypothetical martian scenarios applied on the Iceland fan to illustrate potential limitations of using the final topography to estimate flow dimensions and using a typical value of grain size distribution recorded from Mars missions (as we did in this work). The resulting fan formation timescale was of 0.1–40 h (sand system) and 25–700 h (gravel system), within two orders of magnitude of the real timescale. If sedimentary information is available

FIG. 2. **(A)** Location map of the topographic profiles within the Jezero crater. (**A–B/C–D**) Show the prebreach rim slope; (**E–F**) display outlet channel slope; **(G–H/I–L/M–N)** indicate the inlet (Neretva Vallis) depth at three different locations (a zoom of these profiles is in the Supplementary Data); **(O–Q)** show the delta slope; **(R–S)** show the breach profile with the three main stages in different tones of blue that are described in the main text.

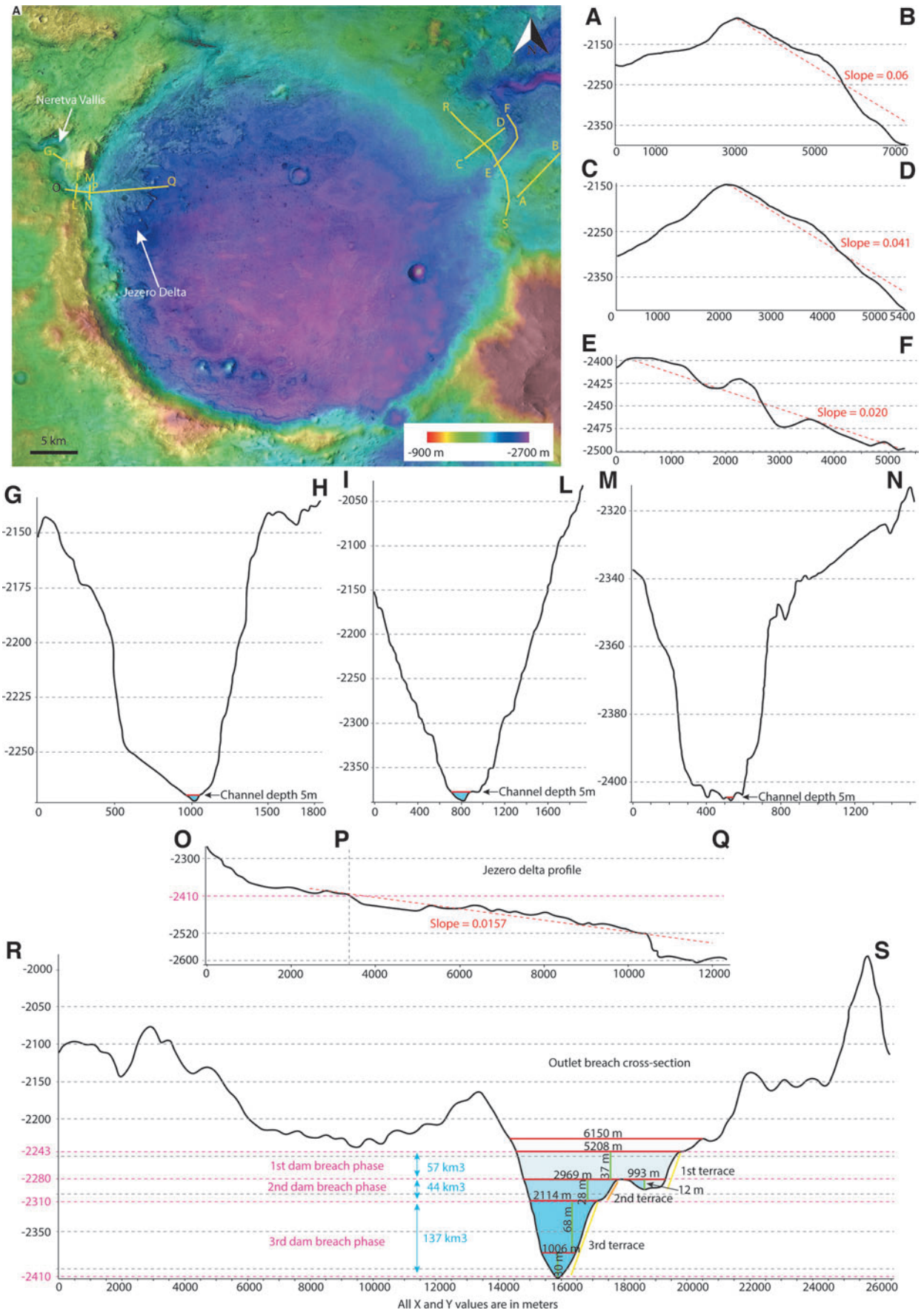

Table 1. List of Parameters and Scenarios Used to Unravel the Timing and Evolution of the Jezero Delta

			Parameters from this work				*Width from Fasset and Head (2005) and Ehlmann* et al. *(2008)*				*Parameters from this work and estimated delta volume of 15 km^3—Delta until remnants (Goudge* et al.*, 2015)*			
Calculation	*Parameters*	*Units*	*1*	*2*	*3*	*4*	*5*	*6*	*7*	*8*	*9*	*10*	*11*	*12*
Input	Channel width	m	190	190	190	190	50	50	50	50	50	50	50	50
	Channel depth	m	5	5	5	5	5	5	5	5	5	5	5	5
	Channel slope	m/m	0.0097	0.0097	0.0097	0.0097	0.0097	0.0097	0.0097	0.0097	0.0097	0.0097	0.0097	0.0097
	Fan-delta slope	m/m	0.0015	0.0015	0.0015	0.0015	0.0015	0.0015	0.0015	0.0015	0.0015	0.0015	0.0015	0.0015
	Fan-delta surface	km^2	30	30	30	30	30	30	30	30	58	58	58	58
	Fan-delta volume	km^3	5	5	5	5	5	5	5	5	15	15	15	15
	Eroded sediment valley volume	km^3	3	3	3	3	3	3	3	3	3	3	3	3
	Basin volume (−2243m)	km3	463.7	463.7	463.7	463.7	463.7	463.7	463.7	463.7	463.7	463.7	463.7	463.7
Sediment transport	Grain size (D50)	m	0.014	0.012	0.01	0.008	0.014	0.012	0.01	0.008	0.014	0.012	0.01	0.008
	Grain size (D90)	m	0.07	0.06	0.05	0.04	0.07	0.06	0.05	0.04	0.07	0.06	0.05	0.04
Discharge calculation	Friction factor	—	0.25	0.25	0.26	0.26	0.25	0.25	0.26	0.26	0.25	0.25	0.26	0.26
	Velocity	m/s	2.4	2.3	2.3	2.3	2.2	2.2	2.2	2.1	2.2	2.2	2.2	2.1
	Froude number	—	0.55	0.54	0.54	0.53	0.51	0.51	0.50	0.50	0.51	0.51	0.50	0.50
	Discharge	km^3/day	2246	2227	2205	2178	553	549	543	537	553	549	543	537
Bed load transport	Shields parameter	—	0.15	0.17	0.19	0.21	0.14	0.15	0.17	0.19	0.14	0.15	0.17	0.19
	Nondimensional transport rate	—	0.34	0.41	0.49	0.63	0.29	0.34	0.42	0.53	0.29	0.34	0.42	0.53
	Volume transport rate	km^3/day	0.0000356	0.0000334	0.0000310	0.0000282	0.00000787	0.00000742	0.00000690	0.00000629	0.00000787	0.00000742	0.00000690	0.00000629
	Water/sediment ratio	—	5458	5755	6140	6663	6078	6395	6808	7372	6078	6395	6808	7372
Total load transport	Shields parameter	—	1.4	1.6	1.9	2.4	1.4	1.6	1.9	2.4	1.4	1.6	1.9	2.4
Suspension dominated	Nondimensional Transport rate	—	0.9	1.3	2.0	3.5	0.9	1.3	2.0	3.5	0.9	1.3	2.0	3.5
	Volume Transport rate	km^3/day	0.0000953	0.0001093	0.0001286	0.0001568	0.0000251	0.0000288	0.0000338	0.0000413	0.0000251	0.0000288	0.0000338	0.0000413
	Water/sediment ratio	—	2037	1760	1482	1200	1907	1649	1388	1124	1907	1649	1388	1124
Formative timescale	Timescale to filling basin until −2243 (H_2O)	years	6.55	6.6	6.65	6.75	26.55	26.76	27.03	27.36	26.55	26.76	27.03	27.36
Formative timescale	Timescale to form delta	years	143.6	125.2	106.5	87.3	545.8	475.8	404.5	331.7	1637.3	1427.4	1213.6	995.0

and used in conjunction with traditional topographic analyses, then the uncertainty in calculating fan formation and hydrologic timescales both on Earth and Mars can be greatly reduced.

As a further independent test of the method, we modeled two recent river-dominated, terrestrial fan deltas for which all the input data are available (including precise start dates of delta formation): the WLD (Louisiana, USA) and the Lake Constance delta (Austria). Input parameters, such as delta bathymetry, channel width and depth, mouth discharge, are all available from existing literature (Muller, 1966; Roberts *et al*., 1997, 2003; Wellner *et al*., 2005; Shaw and Mohrig, 2014; Wessels *et al*., 2015a, 2015b, 2016). The WLD is located in an open, although sheltered, basin with a microtidal range, whereas the New Rhine delta is located in a closed basin (lake).

3. Terrestrial Delta Modeling

3.1. Wax Lake Delta

3.1.1. Sedimentological background. The 25-km-long man-made Wax Lake Outlet was completed in October 1941 (Roberts *et al*., 2003) and provides the opportunity to model a delta formed by a well-developed river with a precisely known initiation date. Wax Lake Outlet extends south from Six Mile Lake, across the Teche Ridge, into Atchafalaya Bay. Original bottom depth was $\sim$13.7 m below mean sea level, and the width was less than 12.2 m (Latimer and Schweizer, 1951). The WLD, at its mouth, is a classic river-dominated delta (Wellner *et al*., 2005; Falcini and Jerolmack, 2010; Edmonds *et al*., 2011), and its form is negligibly affected by the small mean tidal range (0.4 m) and wave climate [0.5 m maximum monthly wave height; Syvitski (2005)]. A delta top slope of 0.0085 was measured from detailed bathymetric reports (Shaw *et al*., (2016).

Researchers have monitored the WLD sedimentation since the works of Morgan *et al*. (1953) and Morgan and Larimore (1957). Roberts *et al*. (1980) suggested that by the late 1950s, accommodation space within the Atchafalaya Basin was rapidly decreasing. The amount of sand-sized sediment reaching the bay consequently increased. Before 1960, the majority of sediment reaching Atchafalaya Bay comprised silt-sized (or finer) grains, with most of this material bypassing the bay and depositing seaward of the Point au Fer Shell reef (Cratsley, 1975). After 1960, sand-prone, subaqueous bayhead deltas formed at the mouths of the Lower Atchafalaya River and Wax Lake Outlet (Roberts *et al*., 1980).

The WLD, according to Cratsley (1975), experienced three different phases of sedimentation: (1) deposition of prodelta clays and silty clays from the middle of the 19th century to about 1952; (2) the initiation of coarser-grained deposition around 1952 (mostly silts), and the development of a lobate form between 1952 and 1962 as reported in the work of Shlemon (1975); and (3) introduction of bed load sands in the early 1970s. Cratsley (1975) also showed that thin silt and sand layers were found in the subaqueous delta and the bulk of the sediments were fine grained and not sand rich.

Deposition between 1962 and 1972, and the high flood years of 1973–1975, which stand out as a period of abnormally high sediment flux, changed bay framework significantly, with the WLD becoming subaerial. Mean discharge and total sediment discharge measured at Simmesport for the years 1951–1989 are summarized in the work of Roberts *et al*. (2003). Majersky *et al*. (1997) showed estimates of delta growth based on a terrain model using both bathymetry and land elevation data collected by the US Army Corps of Engineers. Between 1989 and 1994, the WLD developed at a rate of 3.0 km^2/year (Majersky *et al*., 1997). These values clearly show the rapidly expanding nature of this delta and compare favorably with delta growth predicted earlier by Wells *et al*. (1982) from a genetic growth analysis based on the historic behavior of subdeltas in the modern Mississippi delta, indicating that conditions of flow and sediment transport are within the expected range for this environment.

3.1.2. Modeling. The sediment timescales and delta formation were calculated for conditions shown within the spreadsheet in the Supplementary Data S1. We modeled sediment deposition (delta) between 1952 and 1989 based on variables listed in the work of Roberts *et al*. (2003). Grain size values (D50 and D90) are taken from the work of Shaw and Mohrig (2014). We divided the sedimentary history of this delta into two different periods: silt-dominated before 1961 and sand-dominated after 1961. We found that during the silt-dominated period, the delta formed in 2 years (expected due to the higher mobility of silt). In the sand-dominated period, it formed in almost 13 years. For this case, the calculated timescale is about two factors different from the true timescale (predicted using the spreadsheet: 15 years; reality: 37 years), which is acceptable given all the simplifications and the possible loss of sediment through wave reworking.

3.2. New Rhine delta

3.2.1. Sedimentological background. In 1900 (by a treaty between Austria and Switzerland), the position of the mouth of the Alpine Rhine (Alpenrhein), the upstream reach of the River Rhine, was shifted to a new artificial bed that flows into Fussach Bay (close to the town of Fussach in Austria) in the eastern part of Lake Constance (Muller, 1966). Since then, the Rhine began to build its present delta (the New Rhine delta) into Fussach Bay (Muller, 1966). This provides the opportunity to model a delta formed by a well-developed river with an exactly known initiation date.

The Rhine flows into Lake Constance at an elevation of 396 m above mean sea level. The average gradient between the source of the Vorderrhein and the mouth of the Rhine in Lake Constance (over a total length of about 170 km) is 0.0115. Lake Constance, with a volume of 49.4 km^3 and a maximum depth of 252 m, is the natural settling basin for the Rhine, which drains a total area of 6122 km^2. Over 90% of the coarse sediment transported by the Rhine is deposited in Lake Constance, and only a very small percentage leaves Lake Constance to be carried downstream to the North Sea (Muller, 1966) (making the lake an efficient sediment trap). Fine sediments compose the delta, while the upstream river is gravel-dominated, and the New Rhine transports 85.5% of the suspended load and 1.2% of the bed load (Muller, 1966).

The average water flow discharge from 1931 to 1960 was 224 m^3/s; the average suspended load was 349.5 cm^3/m^3, or 454.1 g/m^3. Thus, the river supplies an average annual

suspended load of 2.571 million m^3, which is deposited into Lake Constance. The amount of bed load (pebbles transported by rolling that constitute less than 2% of the material transported in suspension (Muller, 1966)) is $\sim 40{,}000\,m^3$/year, which is entirely contained within the delta. Seasonal deviations from the average are extreme; during the peak of the thaw period in the Alps, water flow can be 10 times greater, and the amount of suspended load can increase by more than 20 times. Through extension of the delta out into Fussach Bay, the area of Lake Constance has decreased by $\sim 1.2\ km^2$ in 50 years, and the average depth of Fussach Bay has decreased from 17.2 to 4.06 m. The New Rhine delta is composed primarily of silty sands; clean sands and pebble deposits are extremely rare. The average grain size decreases from top-set beds (silty sands) through foreset beds (silty sands and silt) to bottom-set beds (silt to clayey silt that grades into silty clay away from the delta).

3.2.2. Modeling. We modeled sediment deposition of the New Rhine delta for the period between 1900 and 2015. We obtained the morphological and sedimentological parameters from previous studies on Lake Constance and the Alpine Rhine such as those of Muller (1966); Wessels *et al*. (2015a, 2015b); Adami *et al*. (2016); and Wessels *et al*. (2016). In particular, the New Rhine delta volume was calculated by using the 3 m resolution Lake Constance bathymetry constructed by Wessels *et al*. (2015b), with ArcGIS used for volume calculation. The New Rhine delta is a Gilbert-type (Gilbert, 1890). Grain size values (D50 and D90) are taken from the works of Tockner *et al*. (2009) and Adami *et al*. (2016). Input parameters are shown in Section 3.2.1 and in the spreadsheet provided in Supplementary Data S1. For the New Rhine delta, the calculated timescale is again about two factors different from the true timescale (predicted from modeling: 50 years; reality: 115 years), again within the range of expected uncertainty of sediment transport predictions.

4. Jezero Modeling

The morphological elements suggest several possible scenarios of hydrological activity that are discussed in Mangold *et al.* (2020). Based on that discussion, we split the Neretva Vallis evolution history into two phases: phase 1 concerns the basin infilling just after the breaching of the western rim but before delta formation; phase 2 concerns the development of the delta. Herein, we concentrate on the second phase because the first phase is constrained from detailed study by a cover in the crater of presumably volcanic origin. The aim of the modeling is therefore to constrain the period of hydrological activity from (a) observed morphology and (b) flow and sediment transport predictors in the entire active system of inflow, lake, and outflow. All calculations are based on observed volumes and on slopes, widths, and lengths of feeder channels, channels on the delta, and the eastern crater rim breach, as well as on a range of likely grain sizes.

The results of the simulation using relevant Neretva Vallis morphological and sedimentological parameters are shown in Table 1. Considering the volume detailed in Table 1, initially we find out that its suspected filling times (Phase 1) followed a subsequent phase (Phase 2) of delta formation (Kraal *et al*., 2008; Kleinhans *et al*., 2010). Finally, the breach evolution is investigated.

4.1. Phase 1—Basin infilling (full bank + low bank)

We modeled two different scenarios for the Jezero basin infilling phase: one considering Neretva Vallis width and depth calculated in this work and another considering a more conservative (narrower) value of channel width calculated by previous authors (Fassett and Head, 2005; Ehlmann *et al*., 2008). In this work, we estimated Neretva Vallis width of 190 m, channel depth of 5 m, channel slope of 0.0097, and we considered various grain sizes: from pebble to fine sand (Table 1). The time required to fill the basin, considering a continuous flow within a 190-m-wide and 5-m-deep channel, varies between 6.55 and 6.75 years depending on the grain size considered.

4.2. Phase 2—Delta formation

In this section, we show a representative simulation using relevant Jezero morphological and sedimentological parameters listed in Table 1. In particular, we consider a 5 km^3 delta volume as calculated in this study and as suggested by previous researchers (Fassett and Head, 2005; Ehlmann *et al*., 2008). The eroded volume of the final and steepened part of the Neretva Vallis is about 56 km^3 (Mangold *et al.*, 2020), which is far greater than the sediment stored in the fan. We present two main scenarios that differ in channel width value. We again considered different D50 grain sizes from 0.25 to 20 mm (from fine sand to pebble). Morphological parameters used for calculations in both scenarios are listed in Table 1. In that phase, grain size plays a major role for the delta timing; in fact, calculated timescales vary by a factor of 50 depending on whether pebble or fine sands are input. All grain sizes reported hitherto are from distal landing sites [overview in Kleinhans (2005)], and to date, the only genuine measured grain sizes in a fluvio-lacustrine environment on Mars are those reported by Williams *et al*. (2013) measured by the Curiosity rover. We decided to test this model with different grain sizes to show its sensitivity (see spreadsheet in Supplementary Data S2). In the absence of field data and based on the few indications that we have had from the Curiosity rover, in what appears to be a more alluvial environment than fluvial, we preferred to adopt a conservative approach and use the D50 values between 8 and 14 mm to calculate the minimum delta formation time. Calculated timescales for the Jezero delta with the above-mentioned parameters range between 90 and 145 years. By adopting a more conservative channel width value (50 m), estimated by Fassett and Head (2005), and keeping the other parameters unchanged, the delta formation time varies between 330 and 550 years.

A range of 90–550 years for a fan-delta such as Jezero crater do not seem to be an underestimate when compared with the terrestrial case studies. For instance, a progradation rate of 15 m/year was measured by Muller (1966) in the Rhine delta at Constance Lake. For the 5-km-long delta at Jezero, a duration of 100–500 years would correspond to a progradation of 10–50 m/year, consistent with the example at Constance Lake.

There is evidence that the Jezero delta underwent intense erosion at the delta front (Goudge *et al*., 2015), which could

mean a longer formation time if its taken into consideration that the delta extended to the areas where today we only see the remnants of a possible ancient delta front. Goudge *et al*. (2015) estimated a possible eroded delta to have originally been 7.8 km^3 in volume. In this study, we prefer a more conservative estimate and modeled a delta 15 km^3 in volume, which represents the upper limit for the ''delta volume'' parameter in our modeling. For D50 values between 8 and 14 mm (pebble), keeping unchanged the morphological and sedimentological parameters and modifying only the delta volume (from 5 km^3 [real actual delta] to 15 km^3 [delta hypothesized on the basis of the remnants]), the calculated timescale for the Jezero delta then ranges between 260 and 430 years, which is about three times longer than in the modeling of the deposits present today in the crater. If the calculation is conducted with a more conservative width (50 m), then the delta formation time ranges between 1000 and 1640 years.

4.3. Outlet analyses

In this section, we establish whether the processes inherent to the Jezero outlet can further constrain the timescale of hydrological activity. It has previously been established that the sedimentary timescale of fan formation is far larger than the minimum hydrological timescale for the filling of the lake to the topmost level of the delta (Kleinhans, 2005; Kleinhans *et al*., 2010). The topographic gap between the top of the breach and the delta top makes it clear that at some point the lake overflowed. It is possible that lake overflow processes have the ability to do large amounts of erosional and depositional work in a short period of time, especially during the initial phases of dam breaching (Bretz, 1969; O'Connor and Baker, 1992; O'Connor and Beebee, 2009; Roda *et al*., 2014). On Mars, these overflow processes are thought to be characterized by very high discharges and rapid outlet canyon incision (Coleman, 2013, 2015; Roda *et al*., 2014), including incision from multiple lake overflow floods (Salese *et al*., 2016; Goudge *et al*., 2018) and incision from long-term outflow (Holo and Kite, 2017).

The volume of sediment eroded from the rim was estimated using an ArcGIS 10.6 toolbox. This yields an average entire volume of 3 km^3. From the adjacent rim height, it can be estimated that the prebreach paleo-lake level reached at least −2243 m in elevation and the postbreach water surface elevation was estimated as the base of the breach at −2410 m in elevation, which is the same elevation of the Jezero delta top (Fig. 2). The water volume drained from the lake during progressive breach incisions corresponding to the volume contained between −2243 and −2410 m. This yields a minimum water volume of 238 km^3 that must have been expelled from the crater lake during breaching.

The flow flux out of the Jezero crater was likely sediment-poor, ponding water so that the sediment transport capacity of the flow was entirely available for erosion of the channels. This evident water scour is the reverse of the deposition of crater lake deltas from a sediment-laden flow that enters a crater lake (Kleinhans, 2005; Kraal *et al*., 2008) as the gradient of sediment transport integrated over time is the same as the total displaced volume of sediment, allowing the calculation of the timescale (Ts) of formation directly from the volume of displaced sediment ($V = 3$ km^3) and the sediment transport rate (Qs) (corrected for porosity) (Kleinhans, 2005).

The sediment transport rate is calculated from the flow flux through the channel. The following steps were applied to calculate flow flux: (a) width, flow depth, and gradient of the channel are estimated from HRSC topography (Fig. 2a); (b) throughout morphological analyses of the breach, we identified three main terraces that led us to hypothesize at least three different phases within the same event (Fig. 2). These three phases differ in channel depth and width. Furthermore, we model two different breach slope scenarios: (1) considering the slope (0.02) of the actual outlet channel (Fig. 2—Profile E–F); (2) considering a hypothetical prebreach slope (0.05), estimated through the average of the rim slopes to the north and south of the breach. In both cases are steep breaches and in this situation the flow is usually critical (Froude number = 1).

The numerical modeling of crater rim behavior is subject to great uncertainty due to the lack of knowledge about the grain size distribution of materials transported and whether the eroding crust was bedrock, unconsolidated, or comprised weakly cemented sediment. For this reason, we assume a D50 rim grain size of 0.1 m and D90 of 0.6 m, the same values as used for the breach in Aram Chaos from the work of Roda *et al*. (2014). Maximum flow depth is estimated from terrace heights, with hydraulic roughness subsequently calculated.

The water depth inferred from terraces (h) is within the expected range based on the resulting width/depth ratio of the flow (about 20 for narrow terrestrial gravel bed rivers of similar slope) and results in reasonable sediment mobility (expressed as the dimensionless Shields number; Table 2) (Kleinhans, 2005). We assumed near-critical flow (Froude number around 0.9) and use this to confine the water depth. In fact, on such steep slopes, flow is typically critical, resulting in very efficient sediment transport.

We modeled the outlet with parameter settings and choices for independent variables (depth, slope) and the friction relation for these steep slopes. The resulting erosion timescale was always about three orders of magnitude larger than the time needed for the water to flow out of the crater. Unlike the crater breaching case in the work of Roda *et al*. (2014), where the authors apply the same method that we use in this work, there was no reasonable combination of slope, grain size, and friction for which the timescales of water evacuation and breach erosion overlapped. This means that any outflow with erosive power on the crater rim would have emptied the necessary disc of water faster than that flow could have deepened the breach. For the breaching and the delta formation to be coeval, a much larger discharge would be required from the hinterland (in contradiction with outflow calculations).

4.3.1. Outflow evidence implications.

The implication of the timescale calculations is that the breach could not have formed from one overflowing event with the volume of the disc of water, and instead, a much longer process of lake activity and spilling is required. This means that the breach formation was not limited by the amount of water within the lake, but only by the flow discharge from the Neretva Vallis. Furthermore, either the discharge must have been very large to form the breach, or flow must have been acting on the crater wall for a sustained period of time.

Table 2. List of Scenarios for the Three Different Phases of the Jezero Crater Breach

			Scenario Phase 1							
Calculation	*Parameters*	*Units*	*1*	*2*	*3*	*4*	*5*	*6*	*7*	*8*
Input	Channel width	m	4000	4000	4000	4000	4000	4000	4000	4000
	Channel depth	m	5	10	15	20	25	30	35	37
	Channel slope	m/m	0.032	0.038	0.042	0.045	0.048	0.05	0.052	0.053
Discharge calculation	Friction factor	—	0.31	0.37	0.41	0.44	0.47	0.49	0.51	0.52
	Velocity	m/s	3.9	5.5	6.7	7.8	8.7	9.5	10.3	10.6
	Froude number	—	0.9	0.9	0.9	0.9	0.9	0.9	0.9	0.9
	Discharge	km^3/day	6.7	19.0	34.9	53.7	75.1	98.6	124.1	135.0
Bed load transport	Shields parameter	—	0.12	0.19	0.24	0.29	0.34	0.38	0.42	0.44
	Nondimensional transport rate	—	0.23	0.49	0.75	1.05	1.36	1.66	1.96	2.10
	Volume transport rate	km^3/day	0.0094	0.0204	0.0320	0.0440	0.0567	0.0692	0.0821	0.0876
	Water/sediment ratio	—	716	932	1090	1220	1325	1425	1512	1540
Total load transport	Shields parameter	—	0.6	1.5	2.5	3.6	4.8	6.0	7.3	7.8
Suspension dominated	Nondimensional transport rate	—	0.1	0.8	2.4	5.6	10.8	18.0	28.1	33.3
	Volume transport rate	km^3/day	0.004	0.032	0.102	0.232	0.449	0.752	1.173	1.391
	Water/sediment ratio	—	1547	597	342	231	167	131	106	97
Erosion	Sediment breach volume	km^3	3	3	3	3	3	3	3	3
Discharge	Inlet	km^3/day	0.2	0.2	0.2	0.2	0.2	0.2	0.2	0.2
Formative timescale	Timescale to empty the basin until −2410 m	months	0.29	0.10	0.05	0.035	0.025	0.019	0.015	0.014
	Timescale to carve the outlet (suspension dominated)	months	436	60	19	8	4	3	2	1.5
	Timescale to carve the outlet (bed load dominated)	months	202	93	60	43	33.5	27.5	23	22
			Scenario Phase 2							
Calculation	*Parameters*	*Units*	*1*	*2*	*3*	*4*	*5*	*6*	*7*	*8*
Input	Channel width	m	2500	2500	2500	2500	2500	2500	2500	2500
	Channel depth	m	3	9	12	15	18	21	24	28
	Channel slope	m/m	0.028	0.037	0.040	0.043	0.045	0.047	0.049	0.051
Discharge calculation	Friction factor	—	0.28	0.36	0.39	0.42	0.44	0.45	0.47	0.49
	Velocity	m/s	3.0	5.2	6.0	6.8	7.4	8.0	8.6	9.2
	Froude number	—	0.9	0.9	0.9	0.9	0.9	0.9	0.9	0.9
	Discharge	km^3/day	2.0	10.1	15.6	21.9	28.8	36.3	44.3	55.8
Bed load transport	Shields parameter	—	0.09	0.17	0.21	0.24	0.27	0.30	0.33	0.37
	Nondimensional transport rate	—	0.13	0.43	0.60	0.78	0.95	1.13	1.32	1.56
	Volume transport rate	km^3/day	0.0033	0.0113	0.0157	0.0203	0.0248	0.0295	0.0344	0.0408
	Water/sediment ratio	—	597	896	998	1079	1159	1228	1288	1368
Total load transport	Shields parameter	—	0.3	1.3	1.9	2.6	3.2	3.9	4.7	5.7
Suspension dominated	Nondimensional transport rate	—	0.02	0.6	1.3	2.6	4.3	6.8	10.2	15.9
	Volume transport rate	km^3/day	0.004	0.032	0.102	0.232	0.449	0.752	1.173	1.391

(*continued*)

TABLE 2. (CONTINUED)

			Scenario Phase 2							
Calculation	*Parameters*	*Units*	*1*	*2*	*3*	*4*	*5*	*6*	*7*	*8*
	Water/sediment ratio	—	3157	690	459	328	255	204	167	135
Erosion	Sediment breach volume	km^3	3	3	3	3	3	3	3	3
Discharge	Inlet	km^3/day	0.2	0.2	0.2	0.2	0.2	0.2	0.2	0.2
Formative timescale	Timescale to empty the basin until −2410 m (pure water)	months	0.8	0.1	0.09	0.07	0.05	0.04	0.03	0.02
	Timescale to carve the outlet (suspension dominated)	months	3071	129	56	28	17	11	7	4.5
	Timescale to carve the outlet (bed load dominated)	months	581	168	121	94	77	64	55	47

			Scenario Phase 3							
Calculation	*Parameters*	*Units*	*1*	*2*	*3*	*4*	*5*	*6*	*7*	*8*
Input	Channel width	m	4000	4000	4000	4000	4000	4000	4000	4000
	Channel depth	m	5	10	15	20	25	30	35	37
	Channel slope	m/m	0.032	0.038	0.043	0.046	0.05	0.053	0.055	0.057
Discharge calculation	Friction factor	—	0.31	0.37	0.42	0.45	0.48	0.51	0.52	0.54
	Velocity	m/s	3.9	5.5	6.7	7.7	8.7	9.5	10.2	10.6
	Froude number	—	0.9	0.9	0.9	0.9	0.9	0.9	0.9	0.9
	Discharge	km^3/day	2.5	7.1	13.1	20.1	28.1	37.0	46.5	50.7
Bed load transport	Shields parameter	—	0.12	0.18	0.24	0.29	0.34	0.38	0.42	0.44
	Nondimensional transport rate	—	0.22	0.48	0.77	1.05	1.37	1.68	1.98	2.14
	Volume transport rate	km^3/day	0.0035	0.0076	0.0121	0.0165	0.0214	0.0263	0.0311	0.0335
	Water/sediment ratio	—	718	936	1084	1219	1313	1404	1496	1514
Total load transport	Shields parameter	—	0.6	1.5	2.6	3.7	5.0	6.4	7.7	8.4
Suspension dominated	Nondimensional transport rate	—	0.1	0.8	2.6	5.8	11.6	20.2	31.3	38.4
	Volume transport rate	km^3/day	0.002	0.012	0.040	0.091	0.182	0.316	0.491	0.601
	Water/sediment ratio	—	1544	594	326	220	154	117	95	84
Erosion	Sediment breach volume	km^3	3	3	3	3	3	3	3	3
Discharge	Inlet	km^3/day	0.2	0.2	0.2	0.2	0.2	0.2	0.2	0.2
Formative timescale	Timescale to empty the basin until −2410m	months	2	0.7	0.35	0.25	0.16	0.12	0.1	0.09
	Timescale to carve the outlet (suspension dominated)	months	1164	159	47	20	10	6	4	3
	Timescale to carve the outlet (bed load dominated)	months	541	250	157	115	89	72	61	57

On the basis of process knowledge for terrestrial breaches, certain constraints are possible. The large dimensions of the lake (58 km in diameter) mean it is possible to ignore the effects of possible floods or constant flow, as these are buffered by incoming floods and cause limited spilling only (with the exception of some seiches during storms and potential small-scale tsunamis in the aftermath of the crater wall collapse). Regardless of the details, this process must have taken a substantial period of time, or such a large discharge as to be incompatible with the late-stage channel and delta. The breach could not have formed in the same event that formed the present Jezero fan deposit, but must have formed in earlier events associated with the entire channel system to the west (before emplacement of the volcanic layer on the crater floor) (Mangold *et al.*, 2020). During the time needed for delta formation, erosion of the breach is negligible. We therefore assume constant breach elevation and constant lake level during the delta-forming event.

These findings present certain contradictions to previous works as follows: Fassett and Goudge (2017) suggested that most of the flood-related geomorphic work happened within 2 weeks, while Holo and Kite (2017) suggested that the observed outlet can be carved in decades to centuries of progressive bed load as the delta-forming flows filled the lake. Both estimates are problematic given the combination of outflow and sediment transport capacity of that outflow. The Aram Chaos side-channel case, conversely, likely formed in one outflow event because a much larger volume of water became available and the crater rim was far steeper (Roda *et al*., 2014). All such calculations depend on the nature of the sediment, unconsolidated rock, or impact regolith that is eroded [see page 112 on rock and 114 on breaching in the work of Marra *et al*. (2014)].

4.4. Paleo-evaporation rate on Mars and intermittency

The timescale of lake filling would have likely been additionally affected by evaporation. On Earth, 57% of all precipitation on land evaporates, and in warm and dry climates up to 96% of the yearly precipitation may evaporate (Hendriks, 2010). Evaporation is therefore a fundamental parameter in evaluating fluvio-lacustrine lifetimes. On the one hand, high evaporation rates would empty the lake faster following the shutdown of the feeder system. Conversely, given the constraint that the lake must have filled up to the lowest level of the breach in Jezero, evaporation would mean a larger filling timescale with otherwise matching discharge. However, evaporation strongly depends on weather, and any estimates here would therefore invoke significant speculation. There are two widely used methods of estimating evaporation rate for terrestrial systems: (1) pan evaporation; and (2) the more complex but realistic Penman–Monteith equation (Hendriks, 2010).

Pan evaporation is common practice in water resource management for dams and reservoirs. A pan coefficient is applied to measured pan evaporation rates to derive equivalent evaporation from the water storage of interest. This methodology is widely used due to its simplicity, although it results in a number of limitations (Kohler *et al*., 1955; Shuttleworth, 1992; Lowe *et al*., 2009). As stated by Lowe *et al*. (2009), the 95% probability intervals surrounding the estimates of reservoir evaporation on Earth are as large as ±40% of the best estimate using the pan method. Furthermore, one of the main uncertainties of this method is due to pan coefficient itself (Lowe *et al*., 2009), which is between 0 and 1, 0 in the case of warm climate and low humidity and 1 for cold climate and high humidity (Hendriks, 2010). The evaporation from a pan is a good indicator of the evaporation from the surrounding environment only when land surface moisture is in ample supply (Brutsaert, 1982; Brutsaert and Parlange, 1998).

More complex equations, such as the Penman–Monteith equation, are frequently used to estimate evaporation on Earth's open lakes, taking into account the saturation of air flowing over the lake, which acts to reduce evaporation. This approach, while more applicable than pan evaporation on a large lake such as Jezero, requires additional knowledge of several environmental parameters. The main and most important input parameters of these equations are wind speed, air temperature, atmosphere pressure, incoming shortwave radiation, relative humidity, and atmosphere density. While estimates in the literature suggest that evaporation modifies the hydrological timescale as much as grain size changes the sedimentary timescale (Wallace and Sagan, 1979; Sears and Chittenden, 2005; Sears and Moore, 2005), the necessity for variables that are hard to estimate for an early Mars makes it impossible to estimate paleo-evaporation rates with any degree of confidence.

For example, Irwin *et al*. (2015) estimated evaporation rate for the Eberswalde Martian case using pan evaporation. They used a pan coefficient of 0.7 and today's parameters (*e.g.*, solar insolation) to estimate a possible evaporation rate for the martian paleo-environment. This resulted in an evaporation rate range of 0.1–1 m/year. While this is the best estimate possible with what is known for martian conditions, the evaporation rate is based on present meteo-environmental parameters rather than those during the activity of the Eberswalde system, and the obtained value (even for Earth) is large. Note that the greater the temporal duration of a system (*i.e.*, lake), the more significant the value of evaporation rate is for long-term predictions. If the timescale of delta formation was only of the order of years or decades, even such high evaporation would not have significantly modified the order of magnitude of the timescale. We encounter the same issue for the intermittency; if the lake formed in a catastrophic event, then intermittency is not as relevant, but if it took centuries, then it is likely that discharge fluctuated over seasonal or longer time periods.

4.5. Interpretation

Based on the evidence found here and in the companion work of Mangold *et al.* (2020), we can deduce that the long Neretva Vallis (200 km) that drained within the Jezero basin was not entirely related with the present delta. The volume of the missing sediments (56 km^3) within the entire Neretva Vallis is 10 times larger than the present delta volume (5 km^3), even if the remnants are taken into account. The fact that the volume of the delta is almost the same as the eroded sediment volume from the breach is coincidental because the mechanisms cannot be causally linked. Much more likely is the hypothesis that the current delta is linked to flow event(s) that occurred in the relatively late-stage, large valley activity, as well as reliably witnessed by the presence

of knickpoints within the terminal part of the Neretva Vallis (Mangold *et al.*, 2020). Other fluvial sedimentological evidence (*e.g.*, bars) is also apparent upstream. We consider it most probable that flow in the Neretva Vallis would have been shallow, wide, and relatively weak. This is consistent with the findings of the companion article (Mangold *et al.*, 2020): local sediment deposits forming bars but constrained in depth by the rocky valley floor, and a tendency to braid when the valley is wide enough. Furthermore, large discontinuities in channel floor slope suggest that this is not an alluviated equilibrium channel with erodible sediment in the floor, but a bedrock valley formed by an earlier and likely much larger fluvial epoch. The absence of ubiquitous sediment on the valley floor is additional evidence that the

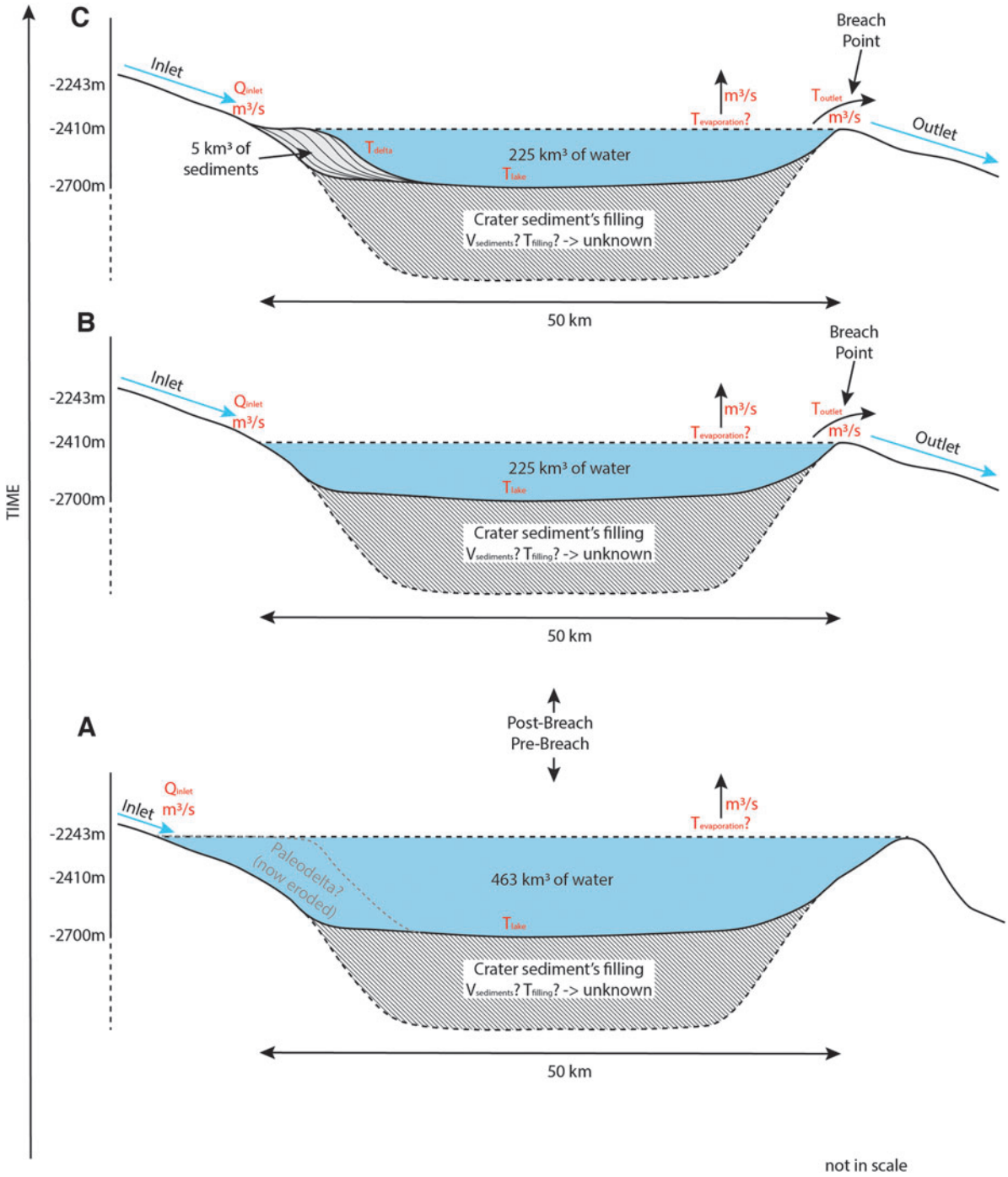

FIG. 3. Proposed model of Jezero basin evolution, independent (black) and dependent (red) variables are indicated in the figure. From the bottom to the top: **(A)** Prebreach stage: the basin was filled at least with 463 km^3 up to –2243 m in elevation. The presence of an older and bigger paleo-delta than we see at present could be supposed but is not considered as there is no evidence of a paleo-delta at this topographic elevation. **(B)** Postbreach phase: the water level drop to –2410 and the water volume within the lake is reduced to 225 km^3. **(C)** Deposition of the Jezero delta. Note that the top of the Jezero delta has the same elevation as the bottom of the breach. See main text for further description.

sediment stored in the delta was either sourced from the sparse cover of loose sediment in the upstream valley system or from erosion of the valley floor immediately upstream of the crater lake.

In Figure 3, we summarize a hypothetical evolution of the Jezero basin. The crater was initially filled by the upstream 200-km-long Neretva Vallis, which acted as a closed basin. At some point, the eastern rim of the crater breached in at least three episodes from −2243 m until −2410 m. From then on, the crater floor transformed into an open lake that filled for a time with sediment-poor water and then started the growth of the Jezero deposits, initially and briefly, according to the evidence of the sediment at the mouth of the Neretva Vallis, as an alluvial fan and later as a delta. Since the top level of the delta is precisely at the level of the breach, the lake probably overflowed and the delta continued to develop for a while longer. Due to the overflowing condition, we cannot constrain an optimum timescale for delta formation by the maximum water level timescale (as is possible for stepped fans). We are more uncertain about the timescale, so we apply a range of grain sizes for a number of channel widths, the main uncertainty in our calculation. We approximate grain size within a logical range (Sklar and Dietrich, 2004; Parker *et al.*, 2007). We have estimates of water depth from the present observations of bar heights, which would have been submerged only during flood, and terraces. Our finding that the sediment timescale is larger than the water timescale is in agreement with our hypothesis, so we end up with the above uncertainty as the range. Then, finally, the lake remains wet, while the upstream feeder system has shut off until the water has percolated/seeped out and/or entirely evaporated. Even if we assume a high evaporation rate of 0.1–1 m/year (Hendriks, 2010), it still adds to the timescale calculation.

4.6. Astrobiological implications for rover exploration

The deposits within the Mars 2020 landing site could have preserved biosignatures that could be investigated on the spot and sampled for a return mission. On Earth, microorganisms have pervaded all wet surface and subsurface environments. In subaqueous environments, microorganisms commonly exist dually in the water column and in sediment pore spaces or as attached biofilms. In addition, sedimentary processing such as hydrodynamic sorting, as is evident in terrestrial fluvial and deltaic environments, may concentrate biologically derived carbonaceous particles into fine-grained, organic-rich horizons in sedimentary beds. Among sedimentary systems on Earth, lacustrine (perennial) and deltaic systems have been estimated as high for supporting organic matter formation, concentration, and preservation (Summons *et al.*, 2011). This is primarily because of the diverse and prolific microbial life that exists in lakes and the existence of hydraulic gradients across deltaic upper plains and slopes, that is, organic material sequestered preferentially by the fine-grained sediments of the distal flood plains and of the bottomsets at the toe of the delta foreslope. By analogy, the deltaic-lacustrine closed basin of western Jezero affords a definite potential for retention of transported and in situ organics and environments that hydrodynamically concentrate organics. Assuming that the lake and delta formed by the processes and on a timescale of decades to millennia (as in our favored interpretation), the following astrobiological implications emerge. In the first place, the gravelly delta itself is an environment poorly favorable to life, because of the high energy in the flow and on the bed. In contrast, it is quite likely that fine-grained sediments were deposited downstream of the delta foreset in bottomsets and on the lake floor. The existence of such fine-grained sediments has been inferred on Mars from lander data, from missing sediment volume in perfectly sediment-trapping crater lakes, and from the ubiquitous fine cover north of the dichotomy (Kleinhans, 2005; Hauber *et al.*, 2013). Such fine-grained sediment potentially provided the nutrients and the low hydrodynamic energy on the lake bed to make this environment astrobiologically significant.

5. Conclusion

The geological and hydrological analyses performed on the Jezero crater and delta deposits indicate that the minimum lake filling timescale with 463 km^3 of sediment-poor water until −2243 m is between 6.55 and 27.36 years depending on the channel width (see spreadsheet in the Supplementary Data S1). The minimum lake delta formation timescale for 5 km^3 up to −2410 m in elevation is 90–150 years with a channel 190 m wide and 330–550 years for a channel 50 m wide. These minimum estimations have been calculated without consideration of intermittency/evaporation/groundwater effects because it is impossible to constrain the impact of these (extinct) processes. The Jezero fan formed as a fluvial delta deposited over a fluvial fan by suspended bed load material, but the timescale uncertainty depends more on unknown grain size than on channel geometry. The discharge of the Neretva Vallis that formed the delta is much smaller than that of the outlet. This confirms that the delta formation and the breach are not coeval because if we compare the two discharges, the basin empties much faster than it fills. Furthermore, the timescale to empty the basin is far smaller than the timescale to carve the breach. This implies that the basin acted as a closed (steady-state) basin for an unknown period of time with a water table at least at −2243 m, and then it had at least three catastrophic collapses or it overflowed for a long (unknown) time such that it carved out the breach. The increase in channel size decreases the duration of the system and further corroborates this hypothesis. The time needed to erode the volume of sediment from the breach (3 km^3), carve the outlet, and remove its 12 km^3 of sediments, compared with the discharge, and the time required to empty the basin suggest a much longer duration of the inlet (Neretva Vallis) or the breach event. The breach, therefore, formed over several distinct events sourced by the channel system upstream of the delta, with the delta itself developing far later.

Our findings with regard to a short duration of formation of the depositional fan of several hundred years do not support the idea of a perennial lake that would have been permissive of the incipience and development of any microbial life. Furthermore, from our analysis, given the high channel discharges, it emerges that the delta toe-set that was dominated by clastic, coarse-deposits (coarse sandstones, conglomerates) is of debatable exobiological significance because of the oxidizing fluids moving through the porous deposits. Conversely, lake floor deposits, paleo-lake margins, and/or delta bottomset are characterized by fine sediments, not trapped in the delta. The latter area is of stronger

exobiological significance than the fan, with the suspended sediment serving as food for potential microscopic life and the lake floor sediment providing a substrate with good preservation potential (*e.g.*, washload sediment settling). However, it should be noted that the Jezero lake may have existed for a long while before this ultimate fluvial gasp, and in the short-in-time, western Jezero fan deposition may have thus initiated into an environment that was already biologically active. The short temporal duration of the system hypothesized from this study does not preclude the possibility of discovering *in situ* organics in the fine-grained deposits, but does reduce the probability of success.

Acknowledgments

The authors thank MRO and HRSC team for these data. Satellite imagery and the Extended Data were generated with ISIS 3 (Integrated Software for Imagers and Spectrometers) available online at (https://isis.astrogeology.usgs.gov). All these data were integrated into ArcGIS 10.6 project. They acknowledge discussions within the rover 2020 team.

Author Disclosure Statement

No competing financial interests exist.

Funding Information

F.S. is supported by the Marie Curie Individual Postdoctoral Fellowship (WET_MARS, Grant Agreement No. 795192). M.G.K. is funded by the European Research Council (ERC Consolidator grant 647570). The data (HRSC, CTX, HiRISE, MOLA) that support the findings of this study were obtained freely from the Planetary Data System (PDS) and are publicly available online at https://pds.nasa.gov/index.shtml. French authors are granted by the Centre National d'Etudes Spatiales (CNES). Région Pays de la Loire through the GeoPlaNet project (Convention No. 2016-10982) also supported this work.

Supplementary Material

Supplementary Data S1
Supplementary Data S2

References

Adami, L., Bertoldi, W., and Zolezzi, G. (2016) Multidecadal dynamics of alternate bars in the Alpine Rhine River. *Water Resour Res* 52:8921–8938.

Adeli, S., Hauber, E., Kleinhans, M., Le Deit, L., Platz, T., Fawdon, P., and Jaumann, R. (2016) Amazonian-aged fluvial system and associated ice-related features in Terra Cimmeria, Mars. *Icarus* 277:286–299.

Adler, J.B., Bell, J.F., Fawdon, P., Davis, J., Warner, N.H., Sefton-Nash, E., and Harrison, T.N. (2018) Hypotheses for the origin of the Hypanis fan-shaped deposit at the edge of the Chryse Escarpment, Mars: is it a delta? *Icarus* 319, 885–908.

Berendsen, H.J.A., and Stouthamer, E. (2000) Late Weichselian and Holocene palaeogeography of the Rhine–Meuse delta, the Netherlands. *Palaeogeogr Palaeoclimatol Palaeoecol* 161:311–335.

Brakenridge, G.R., Newsom, H.E., and Baker, V.R. (1985) Ancient hot springs on Mars—origins and paleoenvironmental significance of small Martian Valleys. *Geology* 13: 859–862.

Bretz, J.H. (1969) The Lake Missoula floods and the channeled scabland. *J Geol* 77:505–543.

Brutsaert, W. (1982) The surface roughness parameterization. In *Evaporation into the Atmosphere*, Springer, Berlin, Germany, pp 113–127.

Brutsaert, W. and Parlange, M.B. (1998) Hydrologic cycle explains the evaporation paradox. *Nature* 396:30.

Coleman, N.M. (2013) Hydrographs of a Martian flood from a breached crater lake, with insights about flow calculations, channel erosion rates, and chasma growth. *J Geophys Res Planet* 118:263–277.

Coleman, N.M. (2015) Hydrographs of a Martian flood from the breach of Galilaei Crater. *Geomorphology* 236:90–108.

Cratsley, D.W. (1975) Recent deltaic sedimentation, Atchafalaya Bay, Louisiana, Unpublished MS thesis, Louisiana State University, Baton Rouge, 142 p.

de Villiers, G., Kleinhans, M.G., and Postma, G. (2013) Experimental delta formation in crater lakes and implications for interpretation of Martian deltas. *J Geophys Res Planets* 118: 651–670.

Di Achille, G. and Hynek, B.M. (2010) Ancient ocean on Mars supported by global distribution of deltas and valleys. *Nat Geosci* 3:459.

Di Achille, G., Ori, G.G., Reiss, D., Hauber, E., Gwinner, K., Michael, G., and Neukum, G. (2006) A steep fan at Coprates Catena, Valles Marineris, Mars, as seen by HRSC data. *Geophys Res Lett* 33. DOI: 10.1029/2005GL025435

Di Achille, G., Ori, G.G., and Reiss, D. (2007) Evidence for late Hesperian lacustrine activity in Shalbatana Vallis, Mars. *J Geophys Res E Planets* 112. DOI: 10.1029/2006JE002858

Duller, R.A., Mountney, N.P., Russell, A.J., and Cassidy, N.C. (2008) Architectural analysis of a volcaniclastic jökulhlaup deposit, southern Iceland: sedimentary evidence for supercritical flow. *Sedimentology* 55:939–964.

Duller, R.A., Warner, N.H., McGonigle, C., De Angelis, S., Russell, A.J., and Mountney, N.P. (2014) Landscape reaction, response, and recovery following the catastrophic 1918 Katla jökulhlaup, southern Iceland. *Geophys Res Lett* 41: 4214–4221.

Duller, R.A., Warner, N.H., De Angelis, S., Armitage, J.J., and Poyatos-More, M. (2015) Reconstructing the timescale of a catastrophic fan-forming event on Earth using a Mars model. *Geophys Res Lett* 42:10324–10332.

Edmonds, D.A., Shaw, J.B., and Mohrig, D. (2011) Topset-dominated deltas: a new model for river delta stratigraphy. *Geology* 39:1175–1178.

Ehlmann, B.L., Mustard, J.F., Fassett, C.I., Schon, S.C., Head, J.W., Marais, D.J.D., Grant, J.A., and Murchie, S.L. (2008) Clay minerals in delta deposits and organic preservation potential on Mars. *Nat Geosci* 1:355–358.

Falcini, F. and Jerolmack, D.J. (2010) A potential vorticity theory for the formation of elongate channels in river deltas and lakes. *J Geophys Res-Earth* 115(F4). DOI: Artn F0403810.1029/2010jf001802

Fassett, C.I. and Goudge, T.A. (2017) Hydrological modeling of the Jezero crater outlet-forming flood [Abstract 1145]. In *Lunar and Planetary Science XLVIII*, Houston, TX, USA.

Fassett, C.I. and Head, J.W. (2005) Fluvial sedimentary deposits on Mars: ancient deltas in a crater lake in the Nili Fossae region. *Geophys Res Lett* 32. DOI: Artn L1420110.1029/2005gl023456

Gilbert, G.K. (1890) *Lake Bonneville*. US Government Printing Office, USA.

Goudge, T.A., Mustard, J.F., Head, J.W., Fassett, C.I., and Wiseman, S.M. (2015) Assessing the mineralogy of the wa-

tershed and fan deposits of the Jezero crater paleolake system, Mars. *J Geophys Res Planet* 120:775–808.

Goudge, T.A., Fassett, C.I., and Mohrig, D. (2018) Characterizing the record of paleolake outlet canyon incision on Mars paper presented at Lunar and Planetary Science Conference.

Halevy, I. and Head, J.W. (2014) Episodic warming of early Mars by punctuated volcanism. *Nat Geosci* 7:865–868.

Hauber, E., Platz, T., Reiss, D., Le Deit, L., Kleinhans, M.G., Marra, W.A., de Haas, T., and Carbonneau, P. (2013) Asynchronous formation of Hesperian and Amazonian-aged deltas on Mars and implications for climate. *J Geophys Res Planets* 118:1529–1544.

Hendriks, M. (2010) *Introduction to Physical Hydrology*. Oxford University Press, USA.

Hill, P.R., Lewis, C.P., Desmarais, S., Kauppaymuthoo, V., and Rais, H. (2001) The Mackenzie Delta: sedimentary processes and facies of a high-latitude, fine-grained delta. *Sedimentology* 48:1047–1078.

Hoke, M.R.T., Hynek, B.M., and Tucker, G.E. (2011) Formation timescales of large Martian valley networks. *Earth Planet Sci Lett* 312:1–12.

Holo, S.J. and Kite, E.S. (2017) *Incision of the Jezero Crater Outflow Channel by Fluvial Sediment Transport*, USA. LPI Contributions, 2014.

Irwin, R.P., Howard, A.D., and Maxwell, T.A. (2004) Geomorphology of Ma'adim Vallis, Mars, and associated paleolake basins. J Geophys Res Planet 109(E12). DOI: Artn E1200910.1029/2004je00228.

Irwin III, R.P., Howard, A.D., Craddock, R.A., and Moore, J.M. (2005) An intense terminal epoch of widespread fluvial activity on early Mars: 2. Increased runoff and paleolake development. *J Geophys Res Planets* 110(E12):1–33.

Irwin, R.P., Lewis, K.W., Howard, A.D., and Grant, J.A. (2015) Paleohydrology of Eberswalde crater, Mars. *Geomorphology* 240:83–101.

Kleinhans, M.G. (2005) Flow discharge and sediment transport models for estimating a minimum timescale of hydrological activity and channel and delta formation on Mars. *J Geophys Res Planet* 110(E12). DOI: Artn E1200310.1029/2005je002521

Kleinhans, M.G., van de Kasteele, H.E., and Hauber, E. (2010) Palaeoflow reconstruction from fan delta morphology on Mars. *Earth Planet Sci Lett* 294:378–392.

Kohler, M.A., Nordenson, T.J., and Fox, W.E. (1955) *Evaporation from Pans and Lakes: US Weather Bureau Research Paper 38.* US Weather Bureau, Washington, DC.

Kraal, E.R., van Dijk, M., Postma, G., and Kleinhans, M.G. (2008) Martian stepped-delta formation by rapid water release. *Nature* 451:973–976.

Latimer, R.A. and Schweizer, C.W. (1951) *The Atchafalaya River Study: A Report Based Upon Engineering and Geological Studies of the Enlargement of Old and Atchafalaya Rivers.* Mississippi River Commission, USA.

Leopold, L.B., Wolman, M.G., and Miller, J.P. (1964) *Fluvial Processes in Geomorphology*. W. H. Freeman and Company, San Francisco.

Lowe, L.D., Webb, J.A., Nathan, R.J., Etchells, T., and Malano, H.M. (2009) Evaporation from water supply reservoirs: an assessment of uncertainty. *J Hydrol* 376:261–274.

Majersky, S., Roberts, H.H., Cunningham, R., Kemp, G.P., and John, C.J. (1997) Facies development in the Wax Lake Outlet delta: present and future trends. *Basin Res Inst Bull* 7:50–66.

Malin, M.C., and Edgett, K.S. (2001) Mars Global Surveyor Mars Orbiter Camera: interplanetary cruise through primary mission. *J Geophys Res-Planet* 106(E10):23429–23570.

Malin, M.C., Bell III, J.F., Cantor, B.A., Caplinger, M.A., Calvin, W.M., Clancy, R.T., Edgett, K.S., Edwards, L., Haberle, R.M., James, P.B., Lee, S.W., Ravine, M.A., Thomas, P.C., and Wolff, M.J. (2007) Context Camera Investigation on board the Mars Reconnaissance Orbiter. *J Geophys Res Planet* 112(E5). DOI: Artn E05s0410.1029/2006je002808

Mangold, N., Kite, E.S., Kleinhans, M.G., Newsom, H., Ansan, V., Hauber, E., Kraal, E., Quantin, C., and Tanaka, K. (2012) The origin and timing of fluvial activity at Eberswalde crater, Mars. *Icarus* 220:530–551.

Mangold, M., Dromart, G., Ansan, V., Salese, F., Kleinhaus, M.G., Massé, M., Quantin, C., and Stack, K.M. (2020) Fluvial regimes, morphometry, and age of Jezero crater paleolake inlet valleys and their exobiological significance for the 2020 Rover Mission Landing Site. *Astrobiology* 20: 994–1013.

Marra, W.A., Braat, L., Baar, A.W., and Kleinhans, M.G. (2014) Valley formation by groundwater seepage, pressurized groundwater outbursts and crater-lake overflow in flume experiments with implications for Mars. *Icarus* 232:97–117.

McEwen, A.S., Eliason, E.M., Bergstrom, J.W., Bridges, N.T., Hansen, C.J., Delamere, W.A., Grant, J.A., Gulick, V.C., Herkenhoff, K.E., Keszthelyi, L., Kirk, R.L., Mellon, M.T., Squyres, S.W., Thomas, N., and Weitz, C.M. (2007) Mars reconnaissance orbiter's high resolution imaging science experiment (HiRISE). *J Geophys Res Planets* 112(E5).

Moore, J.M., Howard, A.D., Dietrich, W.E., and Schenk, P.M. (2003) Martian layered fluvial deposits: implications for Noachian climate scenarios. *Geophys Res Lett* 30(24): 2292, doi: 10.1029/2003GL019002.

Morgan, J.P. and Larimore, P.B. (1957) Changes in the Louisiana shoreline. *Trans Gulf Coast Assoc Geol Soc* 7:303–310.

Morgan, J.P., Van Lopik, J.R., and Nichols, L.G. (1953) *Occurrence and Development of Mudflats Along the Western Louisiana Coast*. Coastal Studies Institute Technical Report No. 2, Louisiana State University.

Muller, G. (1966) The new Rhine delta in Lake Constance. In *Deltas in Their Geologic Framework*, edited by M.L. Shirley and J.E. Ragsdale, Houston Geological Society, Houston, Texas, pp 107–124.

Neukum, G., Jaumann, R., Hoffmann, H., Hauber, E., Head, J.W., Basilevsky, A.T., Ivanov, B.A., Werner, S.C., van Gasselt, S., Murray, J.B., McCord, T.; HRSC Co-Investigator Team (2004) Recent and episodic volcanic and glacial activity on Mars revealed by the High Resolution Stereo Camera. *Nature* 432:971–979.

O'Connor, J.E. and Baker, V.R. (1992) Magnitudes and implications of peak discharges from glacial Lake Missoula. *Geol Soc Am Bull* 104:267–279.

O'Connor, J.E. and Beebee, R.A. (2009) Floods from natural rock-material dams. In *Megaflood Earth Mars*, Cambridge Press, UK, pp 128–163.

Ori, G.G., Marinangeli, L., and Baliva, A. (2000) Terraces and Gilbert-type deltas in crater lakes in Ismenius Lacus and Memnonia (Mars). *J Geophys Res Planets* 105(E7):17629–17641.

Parker, G., Wilcock, P.R., Paola, C., Dietrich, W.E., and Pitlick, J. (2007) Physical basis for quasi-universal relations describing bankfull hydraulic geometry of single-thread gravel bed rivers. *J Geophys Res Earth Surf* 112(F4):1–21.

Pondrelli, M., Rossi, A.P., Marinangeli, L., Hauber, E., Gwinner, K., Baliva, A., and Di Lorenzo, S. (2008) Evolution and

depositional environments of the Eberswalde fan delta, Mars. *Icarus* 197:429–451.

Roberts, H.H., Adams, R.D., and Cunningham, R.H.W. (1980) Evolution of sand-dominant subaerial phase, Atchafalaya Delta, Louisiana. *Aapg Bull* 64:264–279.

Roberts, H.H., Walker, N., Cunningham, R., Kemp, G.P., and Majersky, S. (1997) Evolution of sedimentary architecture and surface morphology. Atchafalaya and Wax Lake Deltas (1973–1994). *Gulf Coast Assoc Geol Soc Trans* 47:477–484.

Roberts, H.H., Coleman, J.M., Bentley, S.J., and Walker, N. (2003) An Embryonic Major Delta Lobe: A New Generation of delta Studies in the Atchafalaya-Wax Lake Delta System. *Gulf Coast Assoc Geol Soc Trans* 53:690–703.

Roda, M., Kleinhans, M.G., Zegers, T.E., and Oosthoek, J.H.P. (2014) Catastrophic ice lake collapse in Aram Chaos, Mars. *Icarus* 236:104–121.

Salese, F., Di Achille, G., Neesemann, A., Ori, G.G., and Hauber, E. (2016) Hydrological and sedimentary analyses of well-preserved paleofluvial-paleolacustrine systems at Moa Valles, Mars. *J Geophys Res Planets* 121:194–232.

Salese, F., Pondrelli, M., Neeseman, A., Schmidt, G., and Ori, G.G. (2019) Geological evidence of planet-wide groundwater system on Mars. *J Geophys Res Planets.* doi: 10.1029/2018JE005802.

Salese, F., McMahon, W.J., Balme, M.R., Ansan, V., Davis, J.M., and Kleinhans, M.G. (2020) Sustained fluvial deposition recorded in Mars' Noachian stratigraphic record. *Nat Commun* 11:2067. https://doi.org/10.1038/s41467-020-15622-0

Schon, S.C., Head, J.W., and Fassett, C.I. (2012) An overfilled lacustrine system and progradational delta in Jezero crater, Mars: implications for Noachian climate. *Planet Space Sci* 67:28–45.

Sears, D.W.G. and Chittenden, J.D. (2005) On laboratory simulation and the temperature dependence of the evaporation rate of brine on Mars. *Geophys Res Lett* 32, L23203, doi: 10.1029/2005GL024154.

Sears, D.W.G. and Moore, S.R. (2005) On laboratory simulation and the evaporation rate of water on Mars. *Geophys Res Lett* 32, L16202, doi: 10.1029/2005GL023443.

Shaw, J.B. and Mohrig, D. (2014) The importance of erosion in distributary channel network growth, Wax Lake Delta, Louisiana, USA. *Geology* 42:31–34.

Shaw, J.B., Ayoub, F., Jones, C.E., Lamb, M.P., Holt, B., Wagner, R.W., Coffey, T.S., Chadwick, J.A., and Mohrig, D. (2016) Airborne radar imaging of subaqueous channel evolution in Wax Lake Delta, Louisiana, USA. *Geophys Res Lett* 43:5035–5042.

Shlemon, R.J. (1975) Subaqueous delta formation—Atchafalaya Bay, Louisiana. *Mar Geol* 214(4):411–430.

Shuttleworth, J.W. (1992) Evaporation. In *Handbook of Hydrology,* edited by D.R. Maidment, McGraw-Hill, New York, pp 4.1–4.53.

Summons, R.E., Amend, J.P., Bish, D., Buick, R., Cody, G.D., Des Marais, D.J., Dromart, G., Eigenbrode, J.L., Knoll, A.H., and Sumner, D.Y. (2011) Preservation of martian organic and environmental records: final report of the Mars Biosignature Working Group. *Astrobiology* 11:157–181.

Sklar, L.S. and Dietrich, W.E. (2004) A mechanistic model for river incision into bedrock by saltating bed load. *Water Resour Res* 40, W06301, doi: 10.1029/2003WR002496.

Syvitski, J.P.M. (2005) The morphodynamics of deltas and their distributary channels. In *River, Coastal and Estuarine Morphodynamics,* edited by G. Seminara and P. Blondeaux, Springer, Berlin, pp 146–153.

Tockner, K., Uehlinger, U., and Robinson, C.T. (2009) *Rivers of Europe*. Academic Press, Elsevier, Netherlands.

Wallace, D. and Sagan, C. (1979) Evaporation of ice in planetary-atmospheres—ice-covered rivers on Mars. *Icarus* 39:385–400.

Weitz, C.M., Irwin, R.P., Chuang, F.C., Bourke, M.C., and Crown, D.A. (2006) Formation of a terraced fan deposit in Coprates Catena, Mars. *Icarus* 184:436–451.

Wellner, R., Beaubouef, R., Van Wagoner, J., Roberts, H.H., and Sun, T. (2005) Jet-plume depositional bodies—the primary building blocks of Wax Lake Delta. *Gulf Coast Assoc Geol Soc Trans* 55:867–909.

Wells, J., Chinburg, S., and Coleman, J.M. (1982) *Development of the Atchafalaya River Deltas: Generic Analysis*, U.S. Army Corps of Engineers, waterways Experiment Station, Vicksburg, MS, 96 p.

Wessels, M., Anselmetti, F., Artuso, R., Baran, R., Daut, G., Gaide, S., Geiger, A., Groeneveld, J.D., Hilbe, M., and Möst, K. (2015a) Bathymetry of Lake Constance—a high-resolution survey in a large, Deep Lake. *Zeitschrift Geodäsie Geoinf Landmanage* 140:203–210.

Wessels, M., Anselmetti, F., Artuso, R., Baran, R., Daut, G., Geiger, A., Gessler, S., Hilbe, M., Möst, K., and Klauser, B. (2015b) Bathymetry of Lake Constance-State-of-the-art in surveying a large lake. *Hydrographischen Nachrichten* 2:6–11.

Wessels, M., Anselmetti, F., Baran, R., Hilbe, M., Gessler, S., and Wintersteller, P. (2016) *Tiefenschärfe–Hochauflösende Vermessung Bodensee*. Internationale Gewässerschutzkommission für den Bodensee (IGKB), Cham, Switzerland.

Williams, R.M.E., Grotzinger, J.P., Dietrich, W.E., Gupta, S., Sumner, D.Y., Wiens, R.C., Mangold, N., Malin, M.C., Edgett, K.S., Maurice, S., Forni, O., Gasnault, O., Ollila, A., Newsom, H.E., Dromart, G., Palucis, M.C., Yingst, R.A., Anderson, R.B., Herkenhoff, K.E., Le Mouélic, S., Goetz, W., Madsen, M.B., Koefoed, A., Jensen, J.K., Bridges, J.C., Schwenzer, S.P., Lewis, K.W., Stack, K.M., Rubin, D., Kah, L.C., Bell III, J.F., Farmer, J.D., Sullivan, R., Van Beek, T., Blaney, D.L., Pariser, O., Deen, R.G.; MSL Science Team. (2013) Martian fluvial conglomerates at Gale Crater. *Science* 340:1068–1072.

Address correspondence to:
Francesco Salese
Faculty of Geosciences
Utrecht University
Princetonlaan 8a
3584 CB, Utrecht
The Netherlands

E-mail: francesco.salese@unich.it

Submitted 15 January 2020
Accepted 16 April 2020

Abbreviations Used

CTX = Context images
DEM = digital elevation model
HiRISE = High Resolution Imaging Science Experiment
HRSC = High Resolution Stereo Camera images
WLD = Wax Lake Delta